

Processing and Properties of Strontium Bismuth Vanadate Niobate Ferroelectric Ceramics

Yun Wu, Chau Nguyen,* Seana Seraji, Mike J. Forbess, Steven J. Limmer, Tammy Chou, and Guozhong Cao*

University of Washington, Materials Science and Engineering, Seattle, Washington 98195

The processing conditions, microstructure, and dielectric properties of strontium bismuth niobate vanadate ceramics, $\text{SrBi}_2(\text{V}_x\text{Nb}_{1-x})_2\text{O}_9$ (SBVN, with $0 \leq x \leq 0.3$), were systematically studied. A relative density of >90% was obtained for all the samples using a two-step sintering process. XRD showed that a single phase with the layered perovskite structure of $\text{SrBi}_2\text{Nb}_2\text{O}_9$ (SBN) was formed with a vanadium content of up to 30 at.%. SEM revealed that the average grain size decreased gradually with an increase in vanadium content. The Curie point was found to gradually increase from $\sim 418^\circ\text{C}$ for SBN to $\sim 459^\circ\text{C}$ for SBVN with 30 at.% vanadium. Dielectric constants at room temperature and their respective Curie points were found to peak at a composition with 10–15 at.% vanadium. Moreover, a high concentration of vanadium (>5 at.%) resulted in a significant increase in tangent loss at low frequencies (<1000 Hz). The relationships between chemical composition, processing condition, microstructure, and dielectric properties of SBVN ferroelectric ceramics are discussed.

I. Introduction

RECENTLY, bismuth-oxide-layered perovskite materials, such as $\text{SrBi}_2\text{Nb}_2\text{O}_9$ (SBN), $\text{SrBi}_2\text{Ta}_2\text{O}_9$ (SBT), and $\text{SrBi}_2(\text{Nb,Ta})_2\text{O}_9$ (SBTN) for FeRAM applications have attracted increasing attention in the research community because they are fatigue-free and lead-free.^{1–3} Moreover, their ferroelectric properties are independent of film thickness and, thus, offer the possibility of fabricating very small devices.⁴ However, the widespread application and commercialization of the bismuth-layered perovskite ferroelectrics have been limited so far mainly by two drawbacks: their rather high processing temperature and their relatively low remanent polarization.^{5,6} There have been many efforts reported recently in the open literature to enhance the properties of layered perovskite ferroelectrics by the addition or substitution of alternative cations. For example, Millan *et al.*^{7–9} studied the substitution of Bi^{3+} in the bismuth oxide layer by other cations, such as Pb^{2+} , Sb^{3+} , and Te^{4+} . It was found that the SBN structure could be preserved by such substitution, and the dielectric properties vary with the substitution of alternative cations. There are many reports on the substitution of A site ions, Sr^{2+} , in the perovskite unit cells, by Bi^{3+} or Ba^{2+} .^{10,11} In general, such substitutions resulted in higher polarization; however, no thorough explanation was given.^{10,11} Recently, Forbess *et al.*¹² have also studied the influence of La^{3+} and Ca^{2+} doping on the dielectric properties of SBN ferroelectric ceramics. It was found that doping with La^{3+} and Ca^{2+} resulted in an appreciable increase in the Curie points and a noticeable

decrease in the dc conductivity. There are also many research reports in the open literature^{13–16} on solid solutions based on the SBTN system. However, few studies can be found on the improvement of ferroelectric properties of the layered perovskite ferroelectrics through substitution of the B site ions (Nb^{5+} or Ta^{5+}) with other alternate cations.

In our previous work,^{17,18} we have proposed and studied the significant enhancement of ferroelectric properties of SBN ferroelectrics through partial substitution of niobium by pentavalent vanadium cations. With 10 at.% vanadium substitution, the remanent polarization increased from ~ 2.4 to $\sim 8 \mu\text{C}/\text{cm}^2$, while the coercive field reduced from ~ 63 to $\sim 45 \text{ kV}/\text{cm}$. The enhanced ferroelectric properties of the layered perovskite ferroelectrics were explained as follows. The partial substitution of Nb^{5+} (ionic radius = 69 pm with CN = 6) with a smaller cation, V^{5+} (58 pm with CN = 6) resulted in an enlarged “rattling space”, which leads to both increased spontaneous polarization and reduced coercive field. Moreover, it was found that the incorporation of vanadium oxide lowered the sintering temperature by $200^\circ\text{--}300^\circ\text{C}$. However, more research needs to be done to get a better understanding of the vanadium-doped-layered perovskite ferroelectrics. For example, it is not known how much vanadium oxide could be incorporated into the crystal structure and how the ferroelectric properties would change with the vanadium concentration. In this paper, we will present a systematic study on the chemical composition, processing conditions, microstructures, and dielectric properties of strontium bismuth niobate vanadate, $\text{SrBi}_2(\text{V,Nb})_2\text{O}_9$, ferroelectric ceramics.

II. Experimental Procedure

Polycrystalline strontium bismuth vanadium niobate ceramic samples with a composition of $\text{SrBi}_2(\text{V}_x\text{Nb}_{1-x})_2\text{O}_9$ (SBVN) with x ranging from 0 to 0.3 (30 at.%) were prepared by two-step solid-state reaction sintering. The starting materials used were SrCO_3 , Bi_2O_3 , V_2O_5 , and Nb_2O_5 (Aldrich Chemical Co., Milwaukee, WI), all with a purity of 99%. The chemicals were admixed with desired ratios with an excess of 4.5 wt% of Bi_2O_3 to compensate for possible weight loss. Details of the sample preparation were described in our previous work,¹⁷ and they are briefly summarized as follows. For all samples, a two-step firing process was applied in this study. The purpose of the first step, calcining at relatively low temperatures ($750^\circ\text{--}1000^\circ\text{C}$), was to promote a chemical reaction among the constituent compounds to form a single-phase layered perovskite. After the first-step calcining, the powders were ground and sieved again for the use of making pellets. The second step, sintering at relatively high temperatures ($800^\circ\text{--}1200^\circ\text{C}$), was to achieve high densification. Before characterization and property measurements, all the samples were annealed in oxygen at 800°C for 3 h.

XRD (Model 1830, Philips, Eindhoven, The Netherlands) was used to determine the formation of the desired layered perovskite phase, for both the powders and the pellets. The XRD spectrum of NaCl crystal was used as a standard to calibrate the scanning angles. The step size of the scan was $0.04^\circ 2\theta$, with a scanning

E. D. Wachsman—contributing editor

Manuscript No. 188748. Received February 10, 2000; approved November 1, 2000.

Supported in part by the Center of Nanotechnology at University of Washington.
*Member, American Ceramic Society.

speed of $0.004^{\circ}2\theta/s$. The pseudotetragonal (200) and (1110) peaks were chosen for the lattice constant calculation, which is commonly used in the calculation of the SBTN system.¹⁹

The microstructure of the sintered sample was analyzed by SEM (Model 5200, JEOL, Peabody, MA) and optical microscopy. Both polished surface and fracture cross section were analyzed, although the SEM images presented in this paper were all made from fracture surfaces.

For the electrical property measurements, the sintered and oxygen annealed pellets were polished to have flat and parallel surfaces. The thickness of the pellets was between 0.25–1 mm. Platinum was sputtered on both sides with a thickness of 300 Å, and then platinum wires were connected to the surfaces with silver paste. The electrodes were then heat-treated on a hot plate at $\sim 500^{\circ}\text{C}$ for 10 min. The dielectric constant and loss tangent, as functions of temperature up to 600°C and frequency ranging from 20 Hz to 1 MHz, were measured by a HP Precision LCR Meter (Model 4284A, Hewlett-Packard, Palo Alto, CA).

III. Results

(1) Sintering Behavior

The two-step sintering process was applied to all the samples studied. The purpose of the first-step sintering (or calcining) was to form a layered perovskite phase at relatively low temperatures (800°C for samples containing a high content of vanadium to 1000°C for the samples without vanadium). The first-step sintering conditions for various samples are summarized in Table I, which also lists the second sintering step conditions used to prepare samples for microstructure and property characterization. A systematic study was performed to find the optimal conditions for the second sintering step and the relative density of the final products as a function of sintering temperatures is summarized in Fig. 1. For all the samples, the overall weight loss was found to be ~ 3 wt%, less than the extra amount of bismuth oxide added into the systems during powder admixing, and is presumably caused by the high vapor pressure of bismuth oxide. No evident relationship between the weight loss and the vanadium content was found; however, the presence of vanadium oxide was seen to promote the densification of the SBVN samples appreciably by lowering the sintering temperatures. Figure 1 clearly indicates that the SBN sample, which contains no vanadium, required a final sintering temperature of $>1200^{\circ}\text{C}$ to achieve a relative density of 90% or above. However, all samples with vanadium doping (from 5 to 30 at.%) were sintered to a relative density of 90% or above, at temperatures as low as 900°C . This is $\sim 300^{\circ}\text{C}$ lower than that of SBN. Vanadium oxide was reported as an effective sintering aid for low-temperature-fired ceramics,²⁰ and the reduction in sintering temperature was generally attributed to the low melting point of vanadium oxide ($\sim 690^{\circ}\text{C}$).²¹ During the first sintering step, or calcining, vanadium oxide reacted with other constituent oxides and formed a layered perovskite (as will be discussed in the following section). There would be very little reacted vanadium oxide left for the second sintering step. Therefore, there might be a very small fraction of liquid phase sintering in the second sintering step. The increase of vanadium concentration from 5 to

Table I. Compositions, Sintering Condition, Relative Density, and Lattice Parameters of the Layered Perovskite SBVN

| Sample | Prefiring | Sintering condition | Relative density |
|---------------------|------------------------------|------------------------------|------------------|
| SBVN ($X = 0$) | 1000°C , 2 h | 1200°C – 2 h | 92% |
| SBVN ($X = 0.05$) | 850°C , 2 h | 950°C – 2 h | 96% |
| SBVN ($X = 0.1$) | 850°C , 2 h | 950°C – 2 h | 91% |
| SBVN ($X = 0.15$) | 850°C , 2 h | 950°C – 2 h | 91% |
| SBVN ($X = 0.2$) | 800°C , 2 h | 900°C – 2 h | 93% |
| SBVN ($X = 0.25$) | 800°C , 2 h | 900°C – 2 h | 91% |
| SBVN ($X = 0.3$) | 800°C , 2 h | 900°C – 2 h | 90% |

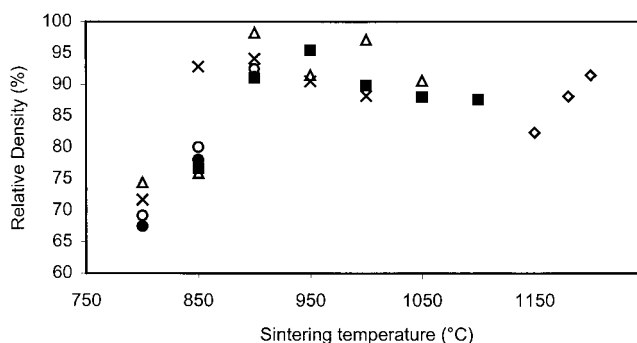


Fig. 1. Densification behavior of the SBVN dielectric ceramic at various sintering temperatures for 2 h in air: (◇) $x = 0$, (■) $x = 0.05$, (△) $x = 0.1$, (×) $x = 0.15$, (○) $x = 0.2$, and (●) $x = 0.25$.

30 at.% was found to have no noticeable influence on the SBVN densification. Moreover, it was found that a high vanadium concentration does not necessarily lead to a higher density.

(2) Formation of Single-Phase Layered Perovskite

XRD analyses (Fig. 2) indicated that single-phase layered perovskites were formed within the composition range studied in this work; no secondary phase was detectable. The lattice constants and single unit cell volumes were calculated from the XRD spectra with NaCl reference peaks (not shown here) and are plotted as a function of vanadium doping (Fig. 3). Figure 3 clearly indicates that the lattice constant, a , does not change with an increasing amount of vanadium content up to 15 at.%; however, a further increase in vanadium content results in a gradual reduction in a . The above dependence of a on the vanadium content can be explained by the limited structural constraint induced by the $[\text{Bi}_2\text{O}_2]^{2-}$ interlayer between the perovskite-like units. With a low concentration of vanadium, although the V^{5+} (58 pm with CN = 6) is significantly smaller than Nb^{5+} (69 pm, CN = 6),²¹ the $[\text{Bi}_2\text{O}_2]^{2-}$ interlayers prevent the shrinkage of the crystal lattice. However, at high vanadium concentrations, the shrinking tendency of the crystal lattice constants overcome the limited structural constraint from the $[\text{Bi}_2\text{O}_2]^{2-}$ interlayers. Therefore, the lattice constant, a , decreases with increasing vanadium concentration. It was noted that the lattice constant, c , showed no noticeable change, although the variation along the c -axis would be less constrained by the $[\text{Bi}_2\text{O}_2]^{2-}$ interlayers. As a result, the unit cell volume

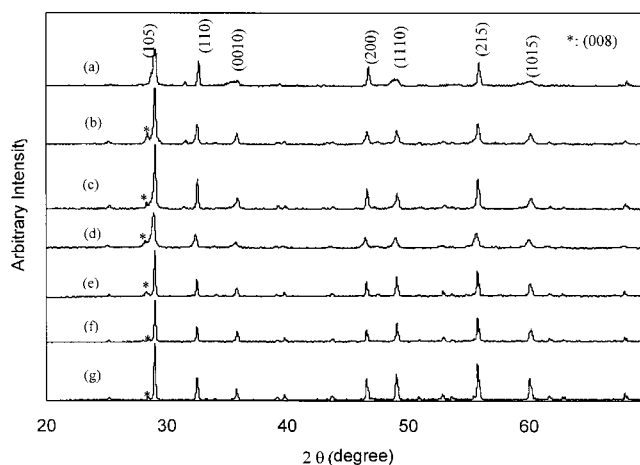


Fig. 2. XRD spectra of the $\text{SrBi}_2(\text{V}_x\text{Nb}_{1-x})_2\text{O}_9$ ferroelectric ceramics: (a) $x = 0.3$, sintered at 900°C for 2 h; (b) $x = 0.25$, sintered at 900°C for 2 h; (c) $x = 0.2$, sintered at 900°C for 2 h; (d) $x = 0.15$, sintered at 950°C for 2 h; (e) $x = 0.1$, sintered at 950°C for 2 h; (f) $x = 0.05$, sintered at 950°C for 2 h; and (g) $x = 0$, sintered at 1200°C for 2 h.

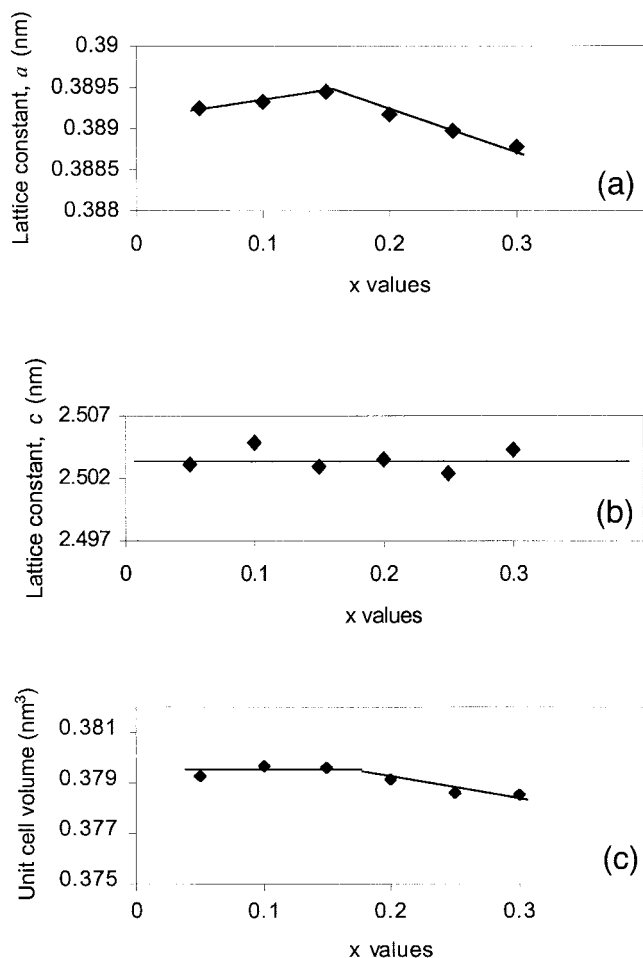


Fig. 3. Lattice constants and unit-cell volumes as a function of vanadium content: (a) lattice constant a ; (b) lattice constant c , and (c) unit-cell volume.

remains unchanged until the vanadium concentration reaches 15 at.%, and then the volume decreases as more vanadium is incorporated into the crystal structure. Also, the current study found that a stable single-phase layered perovskite was formed with up to 30 at.% vanadium doping, although the ionic size difference between Nb^{5+} and V^{5+} is $\sim 19\%$.

(3) Microstructures

Figure 4 shows typical SEM micrographs of fracture surfaces of SBVN ferroelectrics, which consisted of 0, 10, 20, and 30 at.% vanadium, respectively. All samples have a relatively dense structure, although small voids or pores were found in all samples. The SEM images indicate that the SBN samples, consisting of no vanadium, have an average grain size of $\sim 4 \mu\text{m}$, whereas the SBVN samples have a grain size of $\sim 1 \mu\text{m}$. Moreover, a typical intergranular fracture was found. It is noted that the sintering temperature for SBN was $250^\circ\text{--}300^\circ\text{C}$ higher than that of SBVN with vanadium. The smaller grain size might be due to the lower sintering temperature. SBVN samples with a high concentration of vanadium, e.g., with 20 and 30 at.%, had a transgranular fracture surface. This result indicated that the increasing concentration of vanadium led to a stronger connection between and/or better packing of grains. The average grain size of SBVN ferroelectric ceramics is expected to increase if the same sintering conditions were applied. This observation is different from what is commonly found in isotropic perovskite ceramics,²² because the alternate cations may hinder the diffusion across grain boundaries during

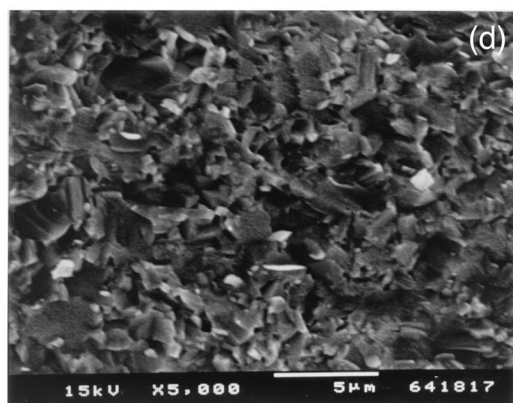
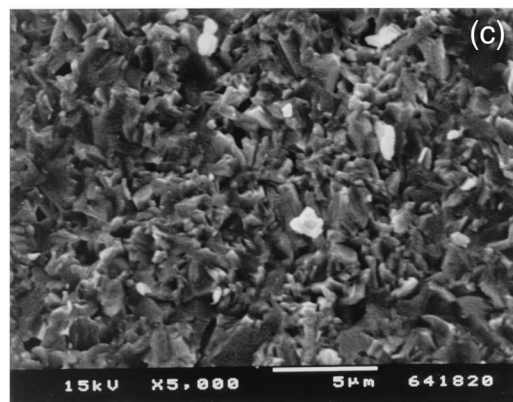
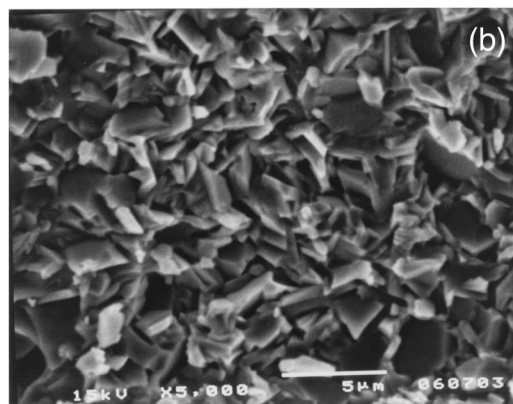
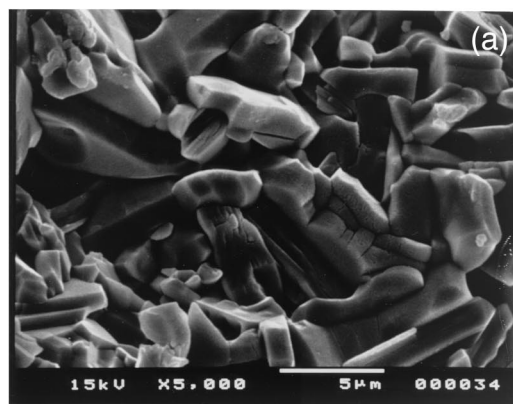


Fig. 4. SEM images showing the fracture surfaces of $\text{SrBi}_2(\text{V}_x\text{Nb}_{1-x})_2\text{O}_9$ ceramics: (a) $x = 0$, (b) $x = 0.1$, (c) $x = 0.2$, and (d) $x = 0.3$.

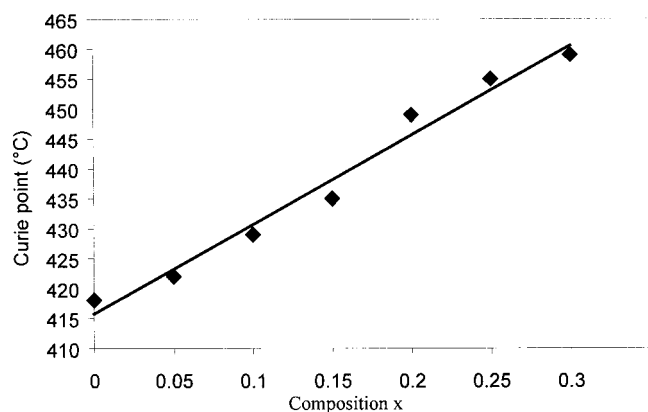


Fig. 5. Curie points of the SBVN ferroelectric ceramics as a function of vanadium concentration.

sintering and, thus, retard the grain growth, resulting in a fine-grained microstructure.

(4) Dielectric Properties

Figure 5 shows the Curie temperature (T_c) as a function of vanadium content. The Curie point gradually increases with increasing vanadium, which could be another indication that a single-phase layered perovskite was formed with up to 30 at.% vanadium substitution. In general, the increase of the Curie point in the system below 15 at.% is mainly caused by the smaller vanadium ions substitution for niobium with an almost unchanged unit cell volume. Above 15 at.%, the increase corresponds to a reduced unit cell volume. The increase in the Curie point shows a slight discontinuity between 15 and 20 at.%, however, no explanation is available. It must be noted that the T_c values are $\sim 20^\circ\text{C}$ lower than what we previously reported,¹⁷ which is because of the different measurement setups used in the previous and current studies.

Figure 6 shows the dielectric constant (not corrected for porosity) as a function of temperature for SBVN ceramics consisting of 0, 10, 20, and 30 at.% vanadium, respectively, determined at a frequency of 100 kHz with an oscillation

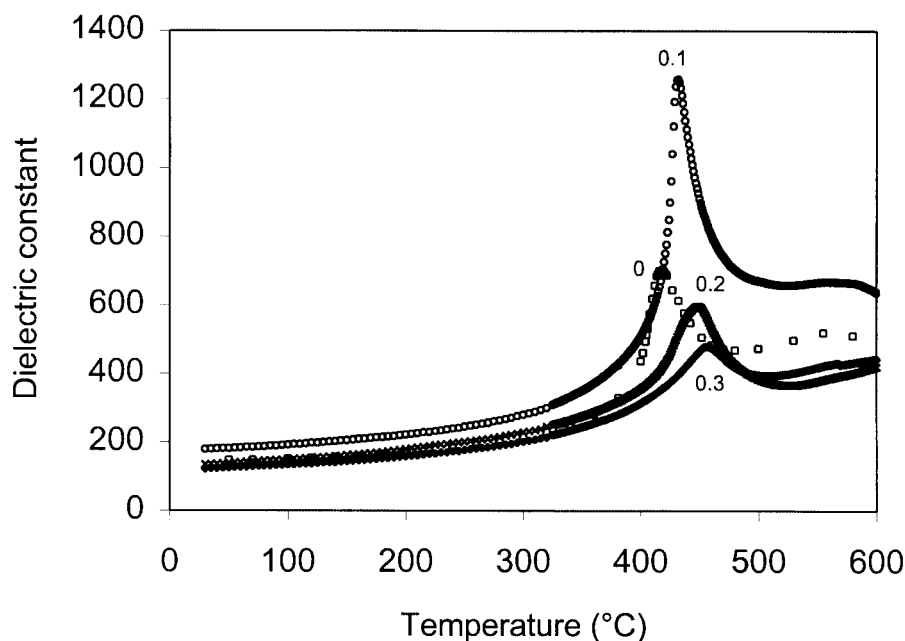


Fig. 6. Dielectric constant as a function of temperature for (\square) $x = 0$, (\circ) $x = 1$, (\times) $x = 0.2$, and (\blacklozenge) $x = 0.3$.

amplitude of 50 mV. For all the samples, there was a sharp transition in dielectric constant at their respective Curie points. It is interesting to note that the dielectric constants of SBVN with 10 at.% vanadium were significantly larger than that of the other three samples. For a better comparison, dielectric constants at both room temperature and their Curie points were plotted as a function of vanadium concentration, as shown in Fig. 7. The dielectric constants at both room temperature and their respective Curie points exhibit similar composition dependence. The dielectric constants were enhanced with the increasing vanadium content up to 15 at.%, and then decreased with a further increasing vanadium content. At higher vanadium concentrations, the dielectric constants at both room temperature and their respective Curie points were lower than that of SBN. Under the measurement conditions (100 kHz and 50 mV) used in the current study, the dielectric constant consists of ionic and atomic polarization only. Because the ionic radius of V^{5+} is smaller than that of Nb^{5+} , an increasing amount of V^{5+} would lead to a reduced electronic polarization. Ionic polarization would be strongly dependent on the lattice constant or unit cell volume. When the concentration of V^{5+} is < 15 at.%, the lattice constants or unit cell volumes remain almost unchanged, as demonstrated in Fig. 3(c). As a result, there would be an increased ionic polarization with an increased V^{5+} concentration, caused by a combination of unchanged unit cell volume and reduced ionic radius. An increase in dielectric constant indicates that the increase in ionic polarization is predominant over the decrease in electronic polarization. However, a higher concentration of vanadium caused a reduction in the lattice constants and unit cell volume (as shown in Fig. 3). As a result, both atomic and ionic polarization would decrease with an increasing amount of vanadium introduced into the system and, therefore, lead to reduced dielectric constants. Moreover, Fig. 7 also shows that the loss tangent at a frequency of 100 kHz remains unchanged with an increasing concentration of vanadium, especially below 15 at.%.

Figure 8 illustrates the dielectric constants and tangent losses as a function of frequency ranging from 20 Hz to 1 MHz at room temperature. The results from four samples were included and the samples consisted of 0, 10, 20, and 30 at.% vanadium, respectively. This figure shows that both dielectric constant and tangent loss for samples consisting of 0 and 10 at.% vanadium have a small variation throughout the frequency range studied.

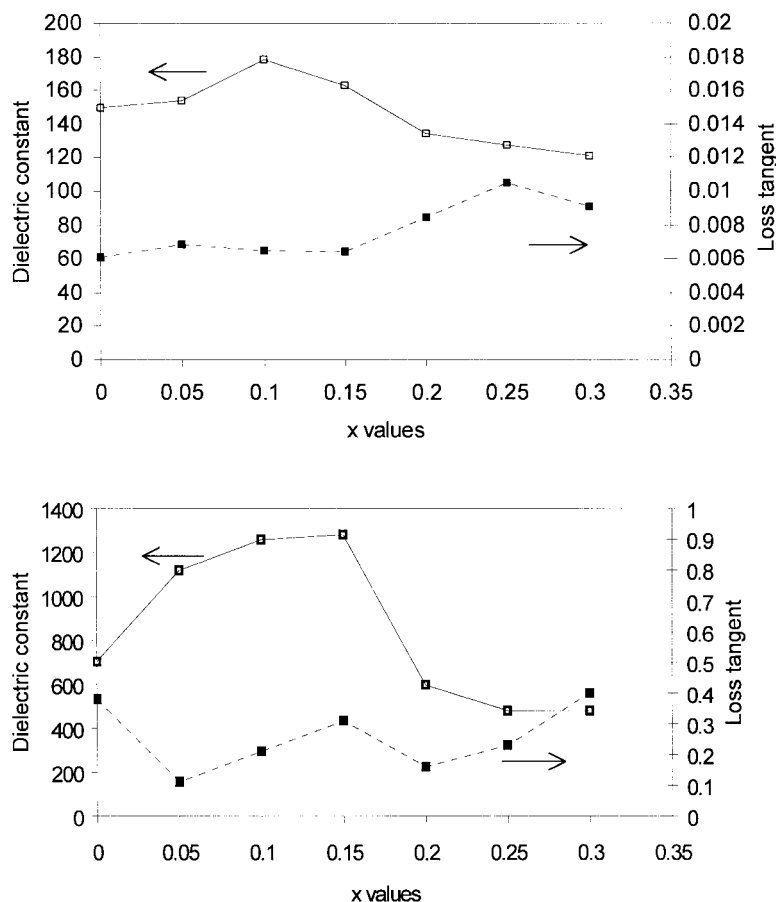


Fig. 7. Dielectric constants and tangent losses as a function of vanadium concentration measured at 100 kHz.

However the other two samples, consisting of 20 and 30 at.% vanadium, show a drastic reduction in both dielectric constant and tangent loss as the frequency increases from 20 Hz to 1 kHz. Under the current experimental conditions (50 mV and 20–1 MHz), there are three possible contributions to dielectric constant: atomic, ionic, and space charge polarization, because the electric field (0.5–2 V/cm) is too small to alter spontaneous polarization. In this system, there would be no dipolar polarization. Response frequencies for atomic and ionic polarization are 10^{15} and 10^{13} Hz, respectively, whereas space charge has a response frequency of ~ 100 Hz. The drastic reduction in dielectric constants, as frequency increases from 20 Hz to 1 kHz, may be attributed to the space charge polarization for $x = 0.2, 0.3$. At frequencies > 1 kHz, space charge polarization no longer exists and, thus, the dielectric constant remains constant as the frequency increases. The loss tangent is caused by space charge and domain wall relaxation. From the above discussion, it is reasonable to assume that the space charge is the main reason for a drastic decrease in tangent loss as the frequency increases from 20 to 1 kHz. Similar high-loss tangent results at a low-frequency range were also seen in bismuth vanadate ceramics.²³ The exact mechanism of increased space charge polarization is not clear; however, it is clear that the high concentration of vanadium is the key factor. More detailed analyses, such as valence state and distribution of vanadium cations, are in progress.

It is well-known that microstructure can have an appreciable influence on the dielectric properties, particularly the dielectric constant.²² In isotropic perovskite ferroelectric ceramics, it was found that the dielectric constant would reach a maximum at a grain size of ~ 1.5 μm in barium titanate ceramics, and decrease with an increased deviation of grain size.^{22,24,25} The present research revealed that the incorporation of vanadium into the

layered perovskite ferroelectric ceramics had appreciable influences on the microstructure. However, the results obtained are obviously insufficient to draw any definitive conclusions on the effects of microstructure on the dielectric properties of layered perovskite ferroelectric ceramics. More detailed and systematic experiments are required to achieve a better understanding of the relationship between the microstructure and dielectric properties.

IV. Conclusion

The incorporation of vanadium oxide was found to greatly promote the densification of SBN ferroelectric ceramics by lowering the sintering temperature of $\sim 300^\circ\text{C}$. A single-phase material with the layered perovskite structure of SBN was obtained with a vanadium concentration up to 30 at.%. Although the ionic radius of V^{5+} was significantly smaller than that of Nb^{5+} , there was no noticeable change in the lattice constants or unit cell volume with a vanadium concentration < 15 at.%. However, a gradual decrease in the unit cell volume was observed with a further increase in vanadium concentration > 15 at.%. The Curie point increased gradually from $\sim 418^\circ\text{C}$ for SBN to $\sim 459^\circ\text{C}$ for SBVN with 30 at.% vanadium. Dielectric constants were found to gradually increase with an increasing concentration of vanadium, reach a maximum at ~ 10 – 15 at.%, and then reduce with a further increase in vanadium concentration. This phenomenon was explained mainly by the variation of ionic polarization caused by the change of unit cell volume as the vanadium concentration increased. Moreover, it was found that a high concentration of vanadium was likely to promote space charge polarization into the system, resulting in a drastic decrease in both dielectric constant and tangent loss as the frequency increased from 20 Hz

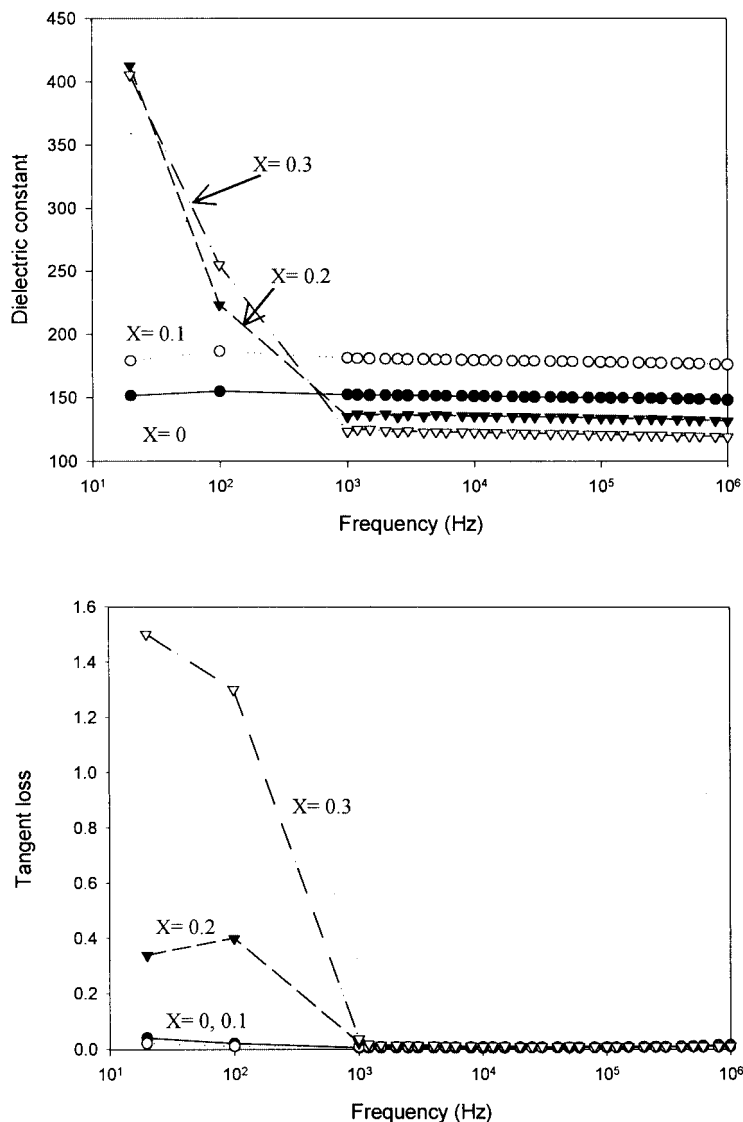


Fig. 8. Dielectric constants and tangent losses of the four typical samples in the SBVN system as a function of frequency at room temperature for (●) $x = 0$, (○) $x = 0.1$, (▼) $x = 0.2$, and (▽) $x = 0.3$.

to 1 kHz. A change in microstructure was seen as the vanadium concentration was increased, although it was difficult to determine the effects of this change on the dielectric properties.

References

- C. A. P. de Araujo, J. D. Cuchiaro, L. D. McMillan, M. C. Scott, and J. F. Scott, "Fatigue-Free Ferroelectric Capacitors with Platinum Electrodes," *Nature (London)*, **374**, 627–29 (1995).
- J. F. Scott and C. A. P. de Araujo, "Ferroelectric Memories," *Science*, **246**, 1400–405 (1989).
- G. Z. Cao, "Ferroelectrics and Applications"; pp. 86–112 in *Advances in Materials Science and Applications*. Edited by D. L. Shi. Tsinghua University Press and Springer-Verlag, Beijing, China, 2001.
- T. Mihara, H. Yoshimori, H. Watanabe, and C. A. P. de Araujo, "Characteristics of Bismuth Layered $\text{SrBi}_2\text{Ta}_2\text{O}_9$ Thin-film Capacitors and Comparison with $\text{Pb}(\text{Zr}, \text{Ti})\text{O}_3$," *Jpn. J. Appl. Phys.*, **34**, 5233–39 (1995).
- J. F. Scott, "Layered Perovskite Thin Films and Memory Devices"; p. 115 in *Thin Film Ferroelectric Materials and Devices*. Edited by R. Ramesh. Kluwer, Norwell, MA, 1997.
- J. F. Scott, "High Dielectric Constant Thin Films for Dynamic Random Access Memories (DRAM)," *Ann. Rev. Mater. Sci.*, **28**, 79–100 (1998).
- P. Duran-Martin, A. Castro, P. Millan, and B. Jimenez, "Influence of Bi-site Substitution on the Ferroelectricity of the Aurivillius Compound $\text{Bi}_2\text{SrNb}_2\text{O}_9$," *J. Mater. Res.*, **13** [9] 2565–71 (1998).
- P. Millan, A. Ramirez, and A. Castro, "Substitutions of Smaller Sb^{3+} and Sn^{2+} Cations for Bi^{3+} in Aurivillius-Like Phases," *J. Mater. Sci. Lett.*, **14**, 1657–60 (1995).
- P. Millan, A. Castro, and J. B. Torrance, "The First Doping of Lead into the Bismuth Oxide Layers of the Aurivillius Oxides," *Mater. Res. Bull.*, **28** [2] 117–22 (1993).
- T. Atsuki, N. Soyama, T. Yonezawa, and K. Ogi, "Preparation of Bi-Based Ferroelectric Thin Films by Sol-Gel Method," *Jpn. J. Appl. Phys.*, **34**, 5096–99 (1995).
- C. Lu and C. Wen, "Preparation and Properties of Barium Incorporated Strontium Bismuth Tantalate Ferroelectric Thin Films," *Mater. Res. Soc. Symp. Proc.*, **541**, 229–34 (1999).
- M. J. Forbess, S. Seraji, Y. Wu, C. P. Nguyen, and G. Z. Cao, "Dielectric Properties of Layered Perovskite $\text{SrBi}_2\text{Nb}_2\text{O}_9$ Ferroelectrics Doped with CaO and La_2O_3 ," *Appl. Phys. Lett.*, **76**, 2934 (2000).
- S. B. Desu and D. P. Vijay, "c-Axis Oriented Ferroelectric $\text{SrBi}_2(\text{Ta}_x\text{Nb}_{2-x})\text{O}_9$ Thin Films," *Mater. Sci. Eng., B*, **32**, 83–88 (1995).
- S. B. Desu and T. Li, "Fatigue-Free $\text{SrBi}_2(\text{Ta}_x\text{Nb}_{1-x})_2\text{O}_9$ Ferroelectric Thin Films," *Mater. Sci. Eng., B*, **34**, L4–L8 (1995).
- K. Kato, C. Zheng, J. M. Finder, S. K. Dey, and Y. Torii, "Sol-Gel Route to Ferroelectric Layer-Structured Perovskite $\text{SrBi}_2\text{Ta}_2\text{O}_9$ and $\text{SrBi}_2\text{Nb}_2\text{O}_9$ Thin Films," *J. Am. Ceram. Soc.*, **81** [7] 1869–75 (1998).
- S. B. Desu, D. P. Vijay, X. Zhang, and B. P. He, "Oriented Growth of $\text{SrBi}_2\text{Ta}_2\text{O}_9$ Ferroelectric Films," *Appl. Phys. Lett.*, **69**, 1719–21 (1996).
- Y. Wu and G. Z. Cao, "Enhanced Ferroelectric Properties and Lowered Processing Temperature of Layered Perovskite by Vanadium Doping," *Appl. Phys. Lett.*, **75**, 2650–52 (1999).
- Y. Wu and G. Z. Cao, "Influences of Vanadium Doping on Ferroelectric Properties of Strontium Bismuth Niobates," *J. Mater. Sci. Lett.*, **15**, 267–69 (2000).
- Y. Torii, K. Tato, A. Tsuzuki, H. J. Hwang, and S. K. Dey, "Preparation and Dielectric Properties of Nonstoichiometric $\text{SrBi}_2\text{Ta}_2\text{O}_9$ -Based Ceramics," *J. Mater. Sci. Lett.*, **17**, 827–28 (1998).

²⁰C. Kuo, C. Chen, and I. Lin, "Microstructure and Nonlinear Properties of Microwave-Sintered ZnO-V₂O₅ Varistors: I, Effect of V₂O₅ Doping," *J. Am. Ceram. Soc.*, **81** [11] 2942–48 (1998).

²¹R.C. Weast and M. J. Astle (Eds.), *CRC Handbook of Chemistry and Physics*, 61st Ed. CRC, Boca Raton, FL, 1974.

²²A. J. Moulson and J. M. Herbert, *Electroceramics*, Chapman and Hall, London, U.K., 1990.

²³K. B. R. Varma and K. V. R. Prasad, "Structural and Dielectric Properties of Bi₂Nb_xV_{1-x}O_{5.5} Ceramics," *J. Mater. Res.*, **11**, 2288 (1996).

²⁴H. T. Marirena and J. C. Burfoot, "Grain Size Effects on Properties of Some Ferroelectric Ceramics," *J. Phys. C: Solid State Phys.*, **7**, 3182–86 (1974).

²⁵U. Kumar, S. F. Wang, S. R. Varanasi, and J. P. Dougherty, "Grain Size Effects on the Dielectric Properties of Strontium Barium Titanate"; pp. 55–60 in *Proceedings of the 8th ISAF*, 1992. □